2. Review Literature

2.1 Anatomy and development of the elbow joint

The elbow joint (cubital joint) is a stable compound ginglymus or hinge joint: It is composed of the humero-radial joint formed by the humeral condyle and head of the radius, the humero-ulnar joint, which is formed by the semilunar notch of the ulna and humeral condyle, and the proximal radio-ulnar joint (FOX et al., 1983; LEWIS et al., 1989; NICKEL et al., 1992; EVANS, 1993; VOLLMERHAUS et al., 1994). The proximal radio-ulnar joint is composed of the articular circumference of the radial head with the radial notch of the ulna (LEWIS et al., 1989). All components share a common joint capsule. The elbow joint enables flexion, extension and a limited amount of rotation. The humero-radial joint is responsible for 75% to 80% of weight-bearing surface of the joint (BERZON and QUICK, 1980) while the humero-ulnar part stabilizes and restricts the movement of the joint in the sagittal plane and the proximal radio-ulnar joint allows rotation of the antebrachium (BERZON and QUICK, 1980; FOX et al., 1983; EVANS, 1993)

The anconeal process of the ulna articulates with the caudal intercondylar surface of the humerus and fits into the supratrochlear fossa when the joint is fully extended. The trochlear notch of the ulna articulates with the trochlear of the humerus. Distal to the trochlear notch are two prominences called the medial and lateral coronoid processes. The medial process is larger and is located more distal than the lateral (BERZON and QUICK, 1980; FOX et al., 1983). Both prominences are articular and act to increase the

total surface area of the elbow joint without contributing to its weight-bearing function (BERZON and QUICK, 1980). The medial prominence or the medial coronoid process (MCP) and the lateral prominence or the lateral coronoid process (LCP) constitute 20% to 25% of the total articular and weight-bearing surface (LJUNGGREN et al., 1966). The radial head articulates with a curved depression between the two coronoid processes called the radial notch and is held in place by the annular ligament (MILLER et al., 1964). The lateral (ulnar) collateral ligament originates on the lateral epicondyle and after blending with the annular ligament divides distally into two crura. The larger cranial portion inserts onto the radial head, while the thinner caudal part inserts in the ulna. A sesamoid bone is occasionally found between the ligament and the radial head (BAUM and ZIETZSCHMANN, 1936). The smaller and weaker medial (radial) collateral ligament originates on the medial epicondyle and also divides into two crura. The weaker cranial part attaches onto the radial head, while the stronger caudal part passes deeply into the interosseous space where it attaches not only to the ulna, but also to the radius (EVANS, 1993). The medial collateral ligament prevents abduction of the elbow joint and the lateral collateral ligament prevents adduction of the elbow joint (GORING and BLOOMBERG, 1983). The annular ligament of the radius is a thin band that runs transversely around the radius. It originates beneath the lateral collateral ligament at the base of LCP and inserts on and below the MCP as it blends with the medial collateral ligament (MILLER et al., 1964). The annular ligament is essential for maintenance of normal articulation between the humerus and the radius and ulna (MILLER et al., 1964; LJUNGGREN et al., 1966). The MCP makes direct contact with the lateral articular surface of the humeral condyle during normal movement of the elbow joint (MILLER et al., 1964; TIRGARI, 1974). Any aberration that would affect

the integrity of these articular surfaces could be a source of severe discomfort (BERZON and QUICK, 1980)

Several separate ossification centers are involved in the development of the elbow joint (HARE, 1961). In the immature elbow, there are six growth plates (BOULAY, 1998). The humeral condyle is formed by two secondary ossification centers: the medial and lateral condyles, which ultimately fuse and possess epicondyle (HARE, 1961; LEWIS et al., 1989). The proximal radius is configured by one secondary ossification center. The proximal ulna, in most instances, has two ossification centers and the anconeal process, which can be radiographically recognized, is formed by one secondary ossification center, in particular, the olecranon apophysis (BOULAY, 1989; MORGAN, 2000). The ossification centers of the anconeal process appear at 12 to 14 weeks and may develop as a direct extension of the diaphysis of ulna or as a separate center of ossification (HARE, 1961; VAN SICKLE, 1966; OLSSON, 1983; GUTHRIE, 1992; TURNER et al., 1998), and at this time, the cartilaginous medial coronoid process begins to ossify from base to its tip and has no separate center of ossification (FOX et al., 1983; OLSSON, 1983; FLÜCKIGER, 1992; GUTHRIE, 1992; BREIT et al., 2004). The ossification of the coronoid process and the fusion of the anconeal process are complete by approximately 16 to 22 weeks (HARE, 1961). In the German Shepherd dog and other large breed dogs the fusion of the anconeal center to the ulna occurs most commonly between the ages of 16 to 20 weeks (VAN SICKLE, 1966; SCHRÖDER, 1978; FOX and WALKER, 1993; SJÖSTRÖM, 1998; TURNER et al., 1998), but in the greyhound between 14 to 15 weeks (VAN SICKLE, 1966). If the anconeal process is not radiographically united at 20 weeks of age, spontaneous union will not occur (FOX et al., 1983; FEHR and MEYER-LINDENBERG, 1992; FOX and WALKER, 1993). We

can see complete ossification of the coronoid process by radiography at the age 20 to 22 weeks (OLSSON, 1983). In some dogs of these breeds, a separate center of ossification may be present in the anconeal process, which unites with the olecranon between the ages of 4 to 6 months. Ossification of the centers of growth occurs early. The medial and lateral condyles of the humerus are first needed to be ossified at 2 to 4 weeks of age and the head of the radius at 3 to 5 weeks of age. The medial epicondyle ossifies later at 6 to 9 weeks. The olecranon ossifies at 7 to 9 weeks (MORGAN, 2000).

WOLSCHRIJN and WEIJS (2004) used microcomputer tomography to evaluate the trabecular alignment within the medial coronoid process and specify the direction of forces within the bone during development. Primary trabecular alignment was found to be perpendicular to the humero-ulnar articular surface in dogs aged four to 24 weeks. This direction is the same as the direction of forces produced by the humero-ulnar joint during weight-bearing. Secondary cranio-caudal alignment corresponding to stresses from the annular ligaments was identified at 13 weeks of age, whereas KÜNZEL et al.(2004) studied the subchondral split line patterns of canine medial coronoid process in bones obtained from 26 deceased large-breed dogs, and determined three main types of split line patterns; the sagittal type, the transverse type, and the intermediate type. These three types corresponded well with the fissure and fragmentation line patterns of the MCP.

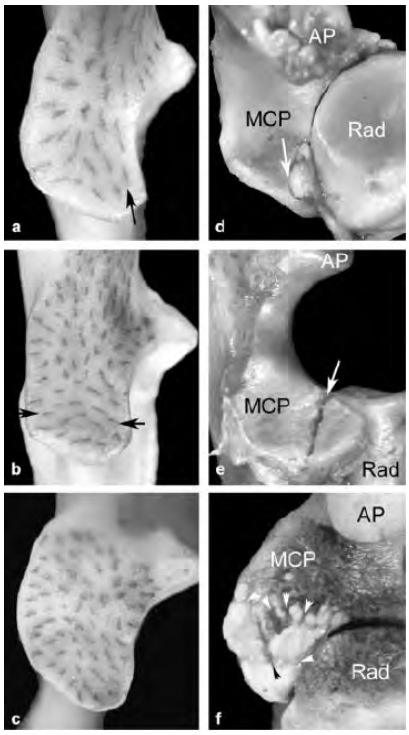

Fig. 1 Split line (a–c) and fragmentation line patterns (d–f) seen in canine ulnae. Note the sagittal alignment of the split lines (black arrow) in (a) characterizing the sagittal type split line was aligned in parallel to the lateral border and at right angles to the rim of the tip and medial border of the MCP. The alignment (black arrows) of split lines in (b) characterizing the transverse type split lines were orientated in a transverse line to both collateral borders (c) representing the intermediate transition type between sagittal and transverse type as the split lines were aligned obliquely to the longitudinal axis of the MCP . Also note similarities in the alignment of the split lines in (a) with the course of the sagittal fragmentation line (white arrow) in (d) showing a left ulna of a male Rottweiler aged 10 years (proximal projection), of the split lines in (b) with the course of the transverse fragmentation line (white arrow) in (e) illustrating the left ulna of a female French bulldog aged 10 years (craniomedial projection), and of the split lines in (c) with the course of the multiple fragmentation lines (arrows) in (f) seen in the left ulna of a male Rough Collie aged 1 year (cranioproximal projection). AP, anconeal process; MCP, medial coronoid process; Rad, radius (KÜNZEL,2004)

2.2 Biomechanics of the elbow joint

The elbow joint is composed of 3 joints; humero-radial, humero-ulnar and proximal radio-ulnar. The humero-radial joint and proximal radio-ulnar joint are simple kinematical joints because they only have one articulation in each joint. The humero-ulnar joint has two contact articulations between the humeral trochlea and the trochlear notch of ulna (THOMSEN et al., 2001). VAN HERPEN (1988) and EVANS (1993) described the three joints of the elbow joint with functions independent of each other. The humero-radial joint carries the bulk of the weight; the humero-ulnar joint causes the strict interaction, and the proximal radio-ulnar joint allows the rotation of the forearm. LIPPERT (1990) also divided the elbow joint of the human being into its three functional part-joints: The humero-ulnar joint is a uniaxial hinge and executes inflection and stretching. The proximal radio-ulnar joint is also a uniaxial joint and executes

bicycle movement: inwards and outwards. The humero-radial joint is a two-axial joint with hinge and rotations, whilst the humero-ulnar joint can rotate only a little (MONTAVON and SALVODELLI, 1995). The lateral collateral ligament and medial collateral ligaments are strongly developed and essentially contribute to the strict interaction within this joint (EVANS, 1993). Adduction and abduction of the joint can be stabilized with two systems. These are comprised of articulation between the humeral trochlea and trochlear notch of the ulna as well as the function of the two ligaments: annular ligament of the radius and collateral ligament (THOMSEN et al., 2001).

The elbow joint is easily bent in the stand-angle. Stand-angles in various dog breeds are German Shepherd 137°, Doberman 138°, Great Dane 159° and Dachshunds 127-124° (MAI, 1995), and the stand-angle in cats is 140° (BRUGGER, 1987). In all breeds the lateral movement-courses are almost completely prevented. Rotation-movements are only possible between radius and ulna. MAI (1995) examined the breeds of German Shepherd, Doberman and German Mastiff and found that the elbow joints of these dogs allow more outside rotation than inside rotation. An exception is in the long haired Dachshund, whose pronation and supination of the elbow joint at the proximal radio-ulnar joint is possible, but the rotation of the radius around the ulna is restricted (NICKEL et al., 1994). While the cat can actively supinate up to 100° (KÖNIG and LIEBLICH, 1999), dogs have only passive supination of movement to approximately 50° and an inward-rotation of approximately 20° (ROOS et al, 1992). As described by RAUSCHER (1986) and EVANS (1993) the dog can supinate about 90° and pronate 45°, although they determined differences with the breed varying from 50° with the supination and 18° with the pronation in the German Shepherd compared to 48° and 28°

in the Dachshund. Some researchers stated that the movement scope of a Dachshund with inflection and stretching amounts to 100°. DOBBERSTEIN and HOFFMANN (1961) concluded that other breeds yielded higher values such as 100° in the Basset, 125° in the German Shepherd and with 140° in the Poodle. VOLLMERHAUS et al. (1994) found that the inflection varied from 60°-70°, while the extension move ranged from 65° to 75°. VAN HERPEN (1988) and EVANS (1993) described three factors which influence the stretching of the elbow joint, namely through the posting of the anconeal process into the olecranon fossa, through the strain of the fore capsule wall and through the passive lengthening-resistance of the flexors. The breaking factors of the inflection are active inflection through a strength, that works from outside, just as the posting of the radial head in the radial fossa.

With reference to the biomechanics of the elbow joint, this joint is compatibility and its function will be achieved if the long growth of ulna and radius is coordinated one on top of the other. The growth of the distal epiphyseal growth plate of the ulna corresponds to the growth of the proximal and distal epiphyseal growth plate of the radius. The growth-performance of the radius equates to around 25 to 40% of the proximal and to 60 to 75% of the distal epiphyseal growth plate (HENSCHEL, 1977; FOX, 1983). The ulna develops around 80 to 85% at the distal epiphyseal growth plate in the long axis; the proximal apophyseal growth plate serves the formation of the olecranon of the ulna and has a growth portion in long of the ulna of 15 to 20% (HENSCHEL, 1977).

WINHART (1991) used Computer Tomography to present the articulating of the proximal joint surface of radius and ulna with the distal joint surface of the humerus on different elbow-joint angles of anatomical preparations and came to the result that by

maximum inflection of the elbow joint only two joints articulate, namely the ulna and the humerus. Moreover, he found that at a higher level of flexion of the elbow joint, the share of the joint surface of ulna is increased while the joint surface of radius is decreased. The critical joint angle in Saint Bernard is 115^{o} and in German Shepherd is 110^{o}.

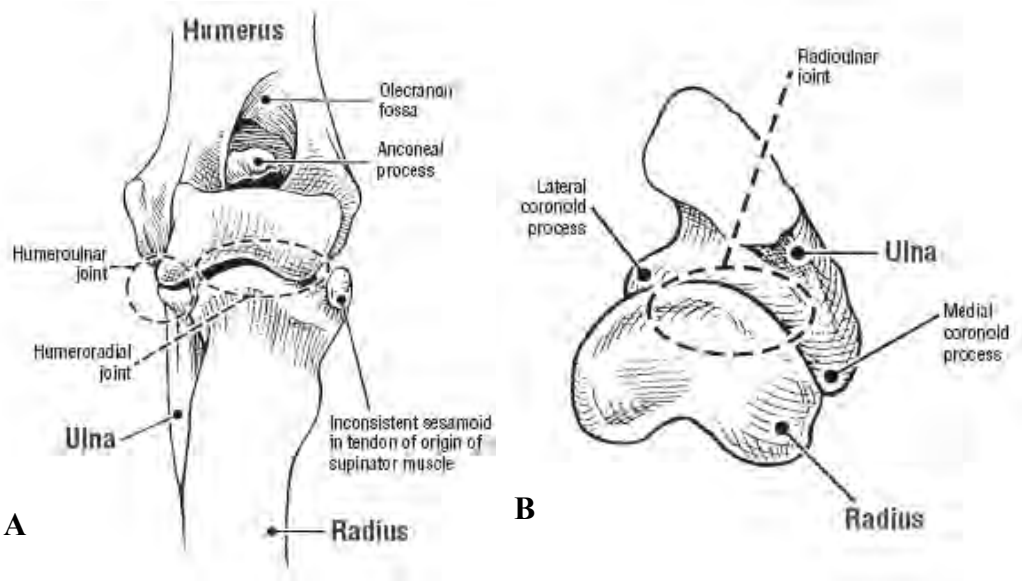

Fig. 2 Cranial projection of the left elbow joint (A) and sagittal projection of the proximal radius and ulna (B). The three separate joints of the elbow are circled. (TROSTEL, 2003)

2.3 Canine Elbow Dysplasia (ED)

2.3.1 Etiology

Canine Elbow Dysplasia (ED), like hip dysplasia, is a relatively widespread problem in different dog breeds. Many authors have assessed the etiology of FMCP and its genetics (GRONDALEN, 1981; GUTHRIE and PIDDUCK, 1990; PADGETT et al., 1995; SWENSON et al., 1997; BEUING et al., 2000; MÄKI et al., 2000; MÄKI et al., 2001) and reported that it can be influenced by external factors such as nutrition and weight gain and physiological factors like asynchronous growth of the radius and ulna

(HEDHAMMER et al., 1974; OLSSON, 1974; GRONDALEN, 1982; BIENZ, 1985; WIND and PACKARD, 1986; GUTHRIE, 1989; ZENTEK et al., 1995).

A genetic cause of FMCP is convincingly argued by the strong breed predispositions associated with the development of the disease (LAFOND et al., 2002). Results of GUTHRIE et al. (1992) and PADGETT et al. (1995) demonstrated that FMCP and OCD did not cosgregate in cross and back crosses of Labrador Retrievers. Some researchers demonstrated that FMCP and incongruity of the elbow joint are independently inherited diseases in Bernese Mountain dogs and FMCP appears to show a polygenic mode of inheritance (PADGETT et al., 1995; UBBINK et al., 1999). Most studies of heritability of the elbow dysplasia have used radiographic scoring for phenotype determination (GUTHRIE, 1989; GUTHRIE and PIDDUCK, 1990; GRONDALEN and LINGAAS, 1991; MÄKI et al., 2000; JANUTTA et al., 2005). However, the heritability of FMCP alone cannot be ascertained from studies using the radiographic assessment of elbow dysplasia (GEMMILL and CLEMENTS, 2007). To the present day, some genomes with relevance to FMCP have been described. SALG et al. (2006) studied in Labrador Retriever and Golden Retriever litters and indicated that FMCP has a sex predisposition occurring in a male to female ratio of 2:1. This is also supported in the other studies (READ et al., 1990; GRONDALEN and LINGASS, 1991). Mutations of the collagen genes are not believed to be a cause of FMCP; however a disturbance of bone modeling together with an overload on the coronoid process may possibly be a cause of FMCP.

2.3.2 Pathogenesis

Recently, three major pathogenic mechanisms were proposed to explain the development of the primary lesions that are discussed here. They are Osteochondritis dissecans (OCD), trochlear notch dysplasia, and asynchronous growth of the radius and

ulna (TROSTEL et al., 2003). Several authors state that either growth retardation of the trochlear notch and radius or ulna leads to elbow joint incongruity. Consequently, developmental incongruence has been hypothesized as a pathogenic mechanism of FMCP due to the increased pressure within the joint (WIND and PACKARD, 1986; MACPHERSON et al., 1992; KIRBERGER and FOURIE, 1998; SAMOY et al., 2006, GEMMILL and CLEMENTS, 2007).

2.3.2.1 Osteochondritis dissecans (OCD)

OLSSON (1993) indicated that almost any acquired defect in the cartilage model that delayed or disrupted endochondral ossification during the skeletal development was an example of OCD. He proposed that the initial lesion of OCD was an acquired defect of chondrocyte differentiation that resulted in faulty cartilage matrix production. The defective matrix would fail to undergo physiologic mineralization, which leads to cartilage necrosis and subsequent fissure formation and fragmentation. Osteochondral fragments may stay in situ or separate from the base of the coronoid process and be displaced (GRONDALEN, 1981). Separated fragments can cause cartilage erosion over the medial coronoid process, 'kissing lesions' on the humeral condyle and secondary osteoarthritis (GRONDALEN, 1981; WIND and PACKARD, 1986; READ et al., 1990; VAN RYSSEN and VAN BREE, 1997; SCHULZ and KROTSCHEK, 2003; MEYER-LINDENBERG and HEINEN, 2004)

OLSSON (1983) indicated that FMCP and Osteochondritis dissecans were manifestations of the OCD complex. The medial coronoid process ossified between 12 to 22 weeks and it is susceptible to any disturbance such as osteochondritis dissecans and mechanical trauma in the deep layers of the cartilage that formed joint surfaces.

This theory has been supported by the reports of GRONDALEN (1981) and WOLSCHRIJN and WEIJS (2005).

However, the theory that the lesions of Canine Elbow Dysplasia are caused by OCD is not supported by consistent findings of histological defective cartilage at early lesion sites (GORING and BLOOMBERG, 1983). A pathoanatomic investigation did not explain the specific locations of OCD on certain joint surfaces or the bilateral pattern of limb involvement of most OCD lesions. Also GRONDALEN (1981) reported finding histological evidence of thickened degenerated cartilage in elbow lesions of less than 20% in the 120 dogs with CED that were included in these studies.

In children, superficial joint surface lesions called transchondral fractures, resemble the articular OCD lesions of animals. They are thought to be caused by traumatic damage to the subchondral capillary bed, which results in ischemia and fractures of the subchondral spongiosa. Mechanical damage leads to the formation of fibrous granulation tissue rather than of osteogenic granulation tissue for endochondral ossification that is necessary for the invasion and replacement of the cartilage model by bone (RESNICK and NIWAYAMA, 1981). OCD of the medial condyle of the humerus in dogs appears similar to these transchondral fractures, and these disorders may have a common pathogenesis (TROSTEL et al., 2003).

POOL (2002) observed in a necropsy study the elbows of immature large breed dogs, and reported that the puppies, which were 3-5 months old, had a compressed subchondral capillary bed, disrupted subchondral spongiosa, and focally thickened cartilage. These lesions were grossly and histologically consistent with OCD lesions (or

transchondral fractures). In puppies older than 5 months of age, focal lesion on the medial humeral condyle were roughened and fibrillated, but had intact articular surfaces.

2.3.2.2 Trochlear notch dysplasia

WIND and PACKARD (1986) studied comparisons between the radiographic and gross necropsy appearance of normal canine elbow joints and FMCP, UAP, and OCD elbow joints in Bernese Mountain dogs. They proposed that in joint incongruity caused by an elliptical trochlear notch, the diameter of the notch was too small to contain the humeral condyle and could result in increased loading at the anconeus process and medial coronoid process. The radiographic appearance of joint incongruity on lateral projection was described in three categories as follows. First, a transient proximal displacement of the trochlear notch of the ulna (up to 3 mm) was detected in puppies 4 to 6 months of age. Second, cranial displacement of the humerus to cranial border of the proximal radius led to increasing humero-ulnar joint space. Third, increased humero-radial joint space developed after the elevation of the medial coronoid process of the ulna and subsequent elevation of the humeral condyle. The resulting malalignment of the proximal part of ulna and radius caused much of the weight that was transferred from the humeral condyle to the antebrachium to be transmitted through the small, elevated medial coronoid process, which caused failure of that small articular process. FMCP resulted from overload, fatigue, and fracture of the medial coronoid process of the ulna. Moreover, the elevated medial coronoid process of the ulna forced the humeral condyle against the anconeal process, which caused trauma to that process. On the other hand VIEHMANN et al. (1999) and COLLINS et al. (2001) found a decreasing radius of the curvature of the cranial aspect of the medial coronoid process in breeds commonly

affected by FMCP when compared with breeds not predisposed to FMCP. This suggests that a mismatch between the radius of curvature of the humeral condyle with respect to the ulnar trochlear notch may be a factor in pathogenesis of FMCP (GEMMILL and CLEMENTS, 2007). Nevertheless, ECKSTEIN et al. (1994) and PRESTON et al. (2000) described that humero-ulnar incongruence might be a normal finding in both human beings and dogs. Necropsy evidence of FMCP dogs was published by WIND and PACKARD (1986). They found that the failure of the developing trochlear notch with respect to the radius of curvature of the humeral condyle can be caused of FMCP. Since the trochlear notch of the ulna is too small to accommodate the humeral trochlea especially in large-breed dogs. It can be concluded that the development of a large olecranon was considered necessary to support the larger muscle mass of the shoulders of these heavy working dogs, and a failed development of the trochlear notch could lead to the proposed incongruence.

2.3.2.3 Asynchronous growth of the radius and ulna

A relative undergrowth of the radius with respect to the ulna may lead to the development of a step defect between the radial head and the coronoid process (WIND and PACKARD, 1986; MORGAN, 2000). BIENZ (1985) performed a radiological survey of 77 Swiss Mountain dogs for ED and recognized the significance of asynchronous growth between the radius and the ulna as the cause of ED in the dogs in this study. SAMOY (2006) indicated that incongruity in case of asynchronous growth of the radius and ulna resulted from a short ulna and a short radius.

In ‘short ulna syndrome’, the humeral condyle has a tight fit between the anconeal process and the radius. This leads to increased pressure on the anconeal process or a

non-union in case of a separate ossification center (VAN SICKLE, 1966). This has been proved by SJÖSTRÖM (1995), who indicated the correlation between a short ulna and an ununited anconeal process. In contrast, MEYER-LINDENBERG et al. (2006) observed 25 dogs with UAP and FMCP. They found that 8 dogs in this study suffered from short ulna syndrome which led to joint incongruity. The remaining 17 dogs had no evidence of incongruity. This study was supported by WIND and PACKARD (1986) who signified that this growth retardation can be compensated at a later stage.

In 'short radius syndrome', WIND and PACKARD (1986) found that the ulna in some of these dogs was temporarily up to 3 mm longer than the paired radius during a vital period of limb development (l6 to 20 weeks of age). This may lead to increase pressure on the medial part of the humeral condyle and the medial coronoid process (KIRBERGER and FOURIE, 1998). Several authors were in agreement with this theory. OLSSON (1981) and MACPHERSON et al. (1992) proved that short radius incongruity can be the cause of lameness and the development of a fragmented coronoid process. In a biomechanics study, PRESTON et al. (2001) elucidated that after shortening the radius, the pressure at the level of the medial coronoid process increases significantly. In contrast, KÖRBEL et al. (2001) demonstrated no difference in loading pressure in joints affected by FMCP when compared to normal joints by CT-absorptiometry.

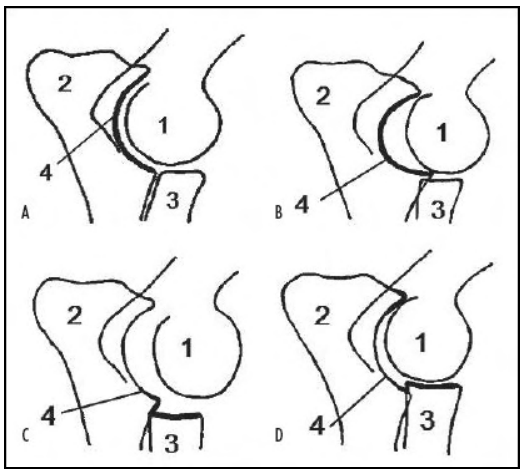

Fig. 3
Alignment of the bones in the elbow. Different forms of incongruity: Schematic drawing.
A) Congruent joint with parallel joint space with 1. humerus, 2. ulna, 3. radius, 4. trochlear notch of the ulna.
B) Incongruent joint with elliptical shape of the trochlear notch instead of round.
C) Incongruent joint with short radius. There is a step in the joint, due to the more distal joint surface of the radius.
D) Incongruent joint with short ulna. There is a step in the joint, due to the more distal joint surface of the ulna. (SAMOY,2006)

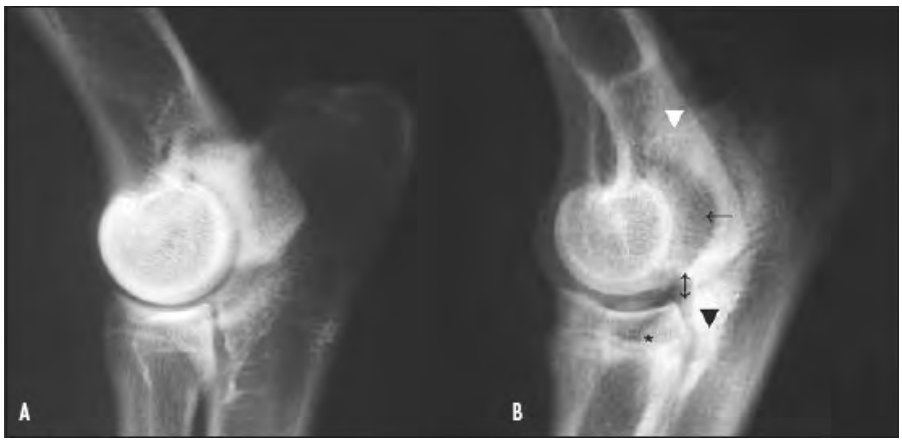

Fig.. 4 A) Mediolateral radiographic projection of a congruent joint.
B) Severe incongruent joint with step (↕) and comma shaped joint space (←). The medial coronoid process (∗) has an irregular aspect. There is arthrosis on the anconeal process (▼) and the proximal part of the radius and there is sclerosis on the trochlear notch (▼). (SAMOY, 2006)

The role of incongruence (trochlear notch dysplasia and asynchronous growth of the radius and ulna) in the development of FMCP has not been clearly defined. However, changing in joint loading, secondary to incongruence, can affect the abnormal development of joint surfaces and can lead to secondary pathologies such as fragmentation of the coronoid process, cartilage erosion and osteoarthritis (GEMMILL and CLEMENTS, 2007).

2.3.3 Diagnostic Imaging Technique of Canine Elbow Dysplasia

Good quality, well-positioned radiographs remain the most cost-effective method of diagnostic elbow dysplasia (KIRBERGER and FOURIE, 1998). Radiographs, however, do not show all abnormalities as are often the case in the growing dog when arthrosis has not yet developed. Three dimensional imaging techniques such as Computer tomography (CT) and Magnetic resonance imaging (MRI) are the most reliable methods, as they allow slices of the affected joint to be evaluated. Linear tomography has also proven to be of benefit. Positive contrast arthrography cannot contribute to the evaluating of FMCP, but can assist in the diagnosis of OCD. Although this technique is easy to perform (LOWRY et al., 1993).

2.3.3.1 Radiography

Optimal radiographic detail is essential to accurately evaluate elbow pathology. This is obtained by using table-top techniques, non-grid exposures, collimating to the elbow joint, centering the primary beam on the medial epicondyle of the humerus, using detail-intensifying screens and short-scale contrast (low kVp and high mAs exposure technique (OLSSON, 1983; GORING and BLOOMBERG, 1983; BERRY, 1992; GUTHRIE et al., 1992). Standard cranio-caudal and mediolateral projections have been supplemented by numerous additional projections in an attempt to highlight certain anatomical locations or pathological conditions. Minor lesions such as erosion of the medial humeral condyle cartilage will not be visible in any of these projections. Microfocal radiography of the elbow has been described and yielded more information than standard radiography, but some lesions were still not detectable, and this is not a readily available technique (KIRBERGER and FOURIE, 1998).

Radiographic findings in FMCP include loss of normal detail in the region of the coronoid process and secondary osteoarthritic changes to the elbow, but the findings often seen are sclerosis of the trochlear notch, and periosteal proliferation of the dorsal anconeal ridge, proximal radius, and medial aspects, of the humerus and ulna. However, the sensitivity of radiographic findings to diagnose FMCP is small even with these special projections (ROBBINS, 1980; OLSSON, 1983; HENRY, 1984; FOX and ROBERTS, 1987; READ et al., 1990; BERRY, 1992; CARPENTER et al., 1993; MEYER-LINDENBERG et al., 2002). Scintigraphy has been reported to be of value as a useful and a sensitive detector of early arthritic changes, but it is expensive and requires hospitalization to contain radioactivity (CHRISTIANSEN et al., 1999). CT permits direct visualization of FMCP but requires general anesthesia. For these reasons, radiography is still the primary screening tool for elbow dysplasia. Direct radiographic visualization of the medial coronoid fragment is uncommon, but the identification of the underlying incongruity or early arthritic changes associated with it can be used with confidence to infer the presence of elbow dysplasia and an FMCP.

The canine elbow is a very complex joint that permits supination and pronation of the antebrachium at all levels of flexion and extension. Diagnosis of elbow dysplasia can be confirmed when FMCP were visualized in radiographic picture but is always difficult to see because the most frequently involved areas of the medial coronoid process are in intimate contact with the radial head and are obscured from projection with planar imaging (HORNOF et al., 2000). Radiography can help diagnose FMCP in most cases. The radiographic projections which should be obtained include a standard lateral, craniocaudal, extended mediolateral, and flexed mediolateral. Extended and supinated caudomedial-craniolateral (Cd75M-CrLO) and craniolateral-caudomedial (Cr15L-

CdMO) projections are also useful in diagnosis of FMCP (ROBBINS, 1980; BERZON and QUICK, 1980; OLSSON, 1983; GORING and BLOOMBERG, 1983; VOORHOUT and HAZEWINKEL, 1987; LEWIS et al., 1989; MIYABAYASHI et al., 1995). Recently, a distomedial-proximo-lateral oblique (Di35M-PrLO) projection was described that also allowed visualization of the medial coronoid region (HAUDIQUET et al., 2002). In many cases, however, a presumptive diagnosis of FMCP is often based on radiographic signs of osteoarthritis.

The advantages and disadvantages in each projection were described by many researchers. The *craniocaudal* projection is the best projection to detect osteochondritis dissecans lesions of the medial humeral condyle (READ et al., 1993). Osteophyte formation at the coronoid process, epicondyle and sesamoid on the annular ligament of the radius can be recognized by this projection. Nevertheless, it is not as useful for detecting subtle lesions associated with elbow dysplasia (TIRGARI, 1974; ROBBINS, 1980; BOUDRIEAU et al., 1983; FEHR and MEYER-LINDENBERG, 1992;). The *craniolateral-caudomedial oblique projection (Cr30^{o}LCdMO)* is also known as the pronated CrCd projection. The beams of x-ray by this projection focus on the medial coronoid process and humeral condyle. For that reason this projection is useful to demonstrate osteophyte reaction on the medial humeral epicondyle and medial coronoid process. Furthermore, osteochondral defects of the medial humeral condyle can be seen in this projection (GRONDALEN, 1979; ROBBINS, 1980; POULOS, 1982; GORING and BLOOMBERG, 1983; PROBST, 1988; FEHR and MEYER-LINDENBERG, 1992; FLÜCKIGER, 1997; MASON et al., 2002). The supinated CrCd, *craniomedial-caudolateral oblique (CrMCdLO) projection*, allowed sight of lateral humeral condyle, sesamoid bone of the annular ligament of the radius, and joint space between the radial

head and medial coronoid process. Moreover, the trochlear notch of the ulna can be detected when the elbow was rotated 25° to x-ray beam (ROBBINS, 1980; BERZON, 1980; MEYER-LINDENBERG, 1990; TELLHEIM, 1991). The recent study by HAUDIQUET et al. (2002) states that abnormal shapes or fragments of the medial coronoid process can be presented by a *distomedial-proximolateral oblique 35 projection*.

Another useful projection to diagnose FMCP is *flexed mediolateral* projection. There are many variations of this projection such as flexed mediolateral with an inside angle of approximately 110°-120° (lateral). This projection allows for the most accurate evaluation of joint incongruity, but true positioning is necessary (READ et al., 1993; KIRBERGER and FOURIE, 1998). The formation of osteophytes or arthrosis at caudal medial/lateral epicondyle can be seen in the flexed mediolateral with maximally flexed projection. Though this projection forces the joint together and can mask joint incongruity or subluxation, it is also difficult to obtain this projection without some degree of superimposition to the humeral condyle, trochlea notch and radial head (OLMSTEAD, 1982; DENNY and GIBBS, 1980; ROBBINS, 1980; BENNETT et al., 1981; OLSSON, 1983; FEHR and MEYER-LINDENBERG, 1992; READ et al., 1993). By supination 5-15° of this joint , good detection cranial contour of the medial coronoid process is achieved (WALDE and TELLHEIM, 1991; GUTHRIE et al., 1991). OCD can be recognized at the humeral condyle, but minor changes may not be detected; besides some authors stated that displacement FPC can be detected by this projection (TIRGARI, 1974; BENNETT et al., 1981; PROBST, 1988; TELLHEIM and SCHLEICH, 1991). Another projection is the flexed mediolateral projection with an inside angle of approximately 45°. This projection maximally exposes the anconeal

process and is optimal for UAP (READ et al., 1993; FLÜCKIGER, 2004). Further mediolateral projection is obtained at *flexed mediolateral with 90^{o}* where detection of osteophyte at the dorsal side of the anconeal process, radial head and at sclerosis at the insertion of trochlear of the ulna is possible. Using this projection UAP, and joint incongruence satisfactory can be well diagnosed (OLSSON, 1975; BERZON, 1980; ROBBINS, 1980; BENNETT et al., 1981; GORING and BLOOMBERG, 1983; BOUDRIEAU et al., 1983; BRUNNBERG and WEIBL, 1986; MURPHY et al., 1998).

2.3.3.2 Computer Tomography

Computer tomography (CT) is a method of acquiring and reconstructing the image of a thin cross section on the basis of measurements of attenuation (HUYGENS and BAERT, 1983; HATHCOCK and STICKLE, 1993). With the discovery of x-rays in 1895, a new era of visualization of internal body structures had begun. This discovery was almost immediately recognized and accepted for its potential as a great medical diagnostic tool. The technique has been characterized by many evolutional improvements during 85 years. In the early 1970s a new technique of x-ray imaging had a revolutionary impact on medicine. In 1971 an x-ray scanner had been developed which produced cross-sectional images of the brain by using several different scientific concepts, some of them known for over 50 years (ROBBINS, 1982). In comparison with the conventional radiographs, CT images are free of superimposing tissues and are capable of much higher contrast due to the elimination of scatter. The tomography nature of CT images provides accurate anatomic evaluation of tissue planes and regions which are often impossible to visualize with conventional radiography. The most valuable property of this new technique is its high contrast resolution. The ability to image in cross-section makes it possible to build up a three-dimensional picture, which

is invaluable for understanding normal anatomy and for planning surgical or radiotherapy treatment. The greatly increased tissue resolution allows differentiation between fluid and solid tissues and assessment of the internal structure of soft tissues (DENNIS, 1995).

2.3.3.2.1 Image Formation

In conventional radiography, a broad x-ray beam is emitted from a stationary tube and passes through the patient, casting a shadow on a flat screen that absorbs the x-rays and then re-emits their energy as light, which affects photographic film. In CT, a narrow, fan shaped x-ray beam is emitted from a tube as it moves around the patient, and x-rays that pass through the patient are counted by a series of small electronic detectors; signals from the detectors are then passed to a computer, which reconstructs the data into a two-dimensional image representing a cross-section of the patient (KALENDER, 2000). The CT scanner represents a high-quality piece of engineering that includes a high-output x-ray tube, a gantry that supports the x-ray tube, detector array, and a patient bed. The operation of the scanner is controlled by a computer. CT images are viewed as they are acquired on a monitor. Other scans can be viewed or manipulated on a remote workstation without interfering with the scan in progress. CT images can be printed onto film so that they may be viewed on a light box. During a scan, the x-ray tube normally revolves continuously through 360° around the patient as the patient is moved through the aperture of the scanner; the patient is moved either in a series of small increments (axial scan mode) or continuously (helical scan mode). The size of the region and the thickness of tissue represented by each image can be precisely selected by the radiographer. Thin slices (i.e. 1 to 2 mm) of the patient can be obtained when maximal resolution of small, high-contrast structures is prescribed (e.g. when examining the bones of the middle and inner ear). As an alternative, thicker slices (i.e. 5 to 8 mm) can be

used when it is important to distinguish between tissues of similar attenuation (e.g. parts of the brain, abdominal organs). Thicker slices are necessary because recognition of small differences in attenuation (i.e. low contrast resolution) depends mainly on minimizing statistical variations (i.e. “noise”) in the images; this is achieved by using thicker slices with a correspondingly higher radiation dose (HATHCOCK and STICKLE, 1993; KALENDER, 2000; FEENEY et al., 2001; WHATMOUGH and CHRISTOPHER, 2006). CT scans have properties similar to those of conventional radiographs because both are produced via the absorption of x-rays by tissues of different density; thus low-density tissues (e.g. lungs) appear black or dark grey, and high-density tissues (e.g. bone) appear light grey or white. The major differences between conventional radiographs and CT images are: first, a CT image represents thinner sections of the patient than radiography. Therefore, it takes more time to cover a particular anatomic structure or body cavity. Second, CT images are digital and composed of many pixels, each with a number that describes the attenuation of the tissue within that pixel, and the last difference is CT images display the attenuation directly assigned to each pixel, whereas conventional radiographs present the sum of attenuations within all superimposed structures within the thickness of the patient. CT can detect differences in tissue density that are too small to be visible on conventional radiographs (KALENDER, 2000, WHATMOUGH and CHRISTOPHER, 2006).

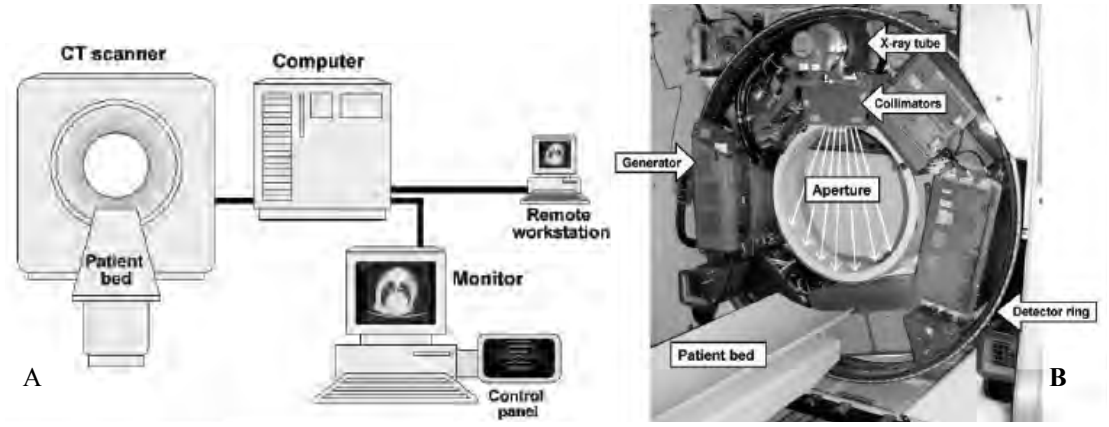

Fig. 5 (A) The components of a typical CT system. In addition, images may be sent to a printer or archived via a radiology information system to an image server (not shown). (B) A CT scanner with the front cover removed during installation. The *arrows* in the aperture indicate the direction of the x-ray beam. (WHATMOUGH, 2006)

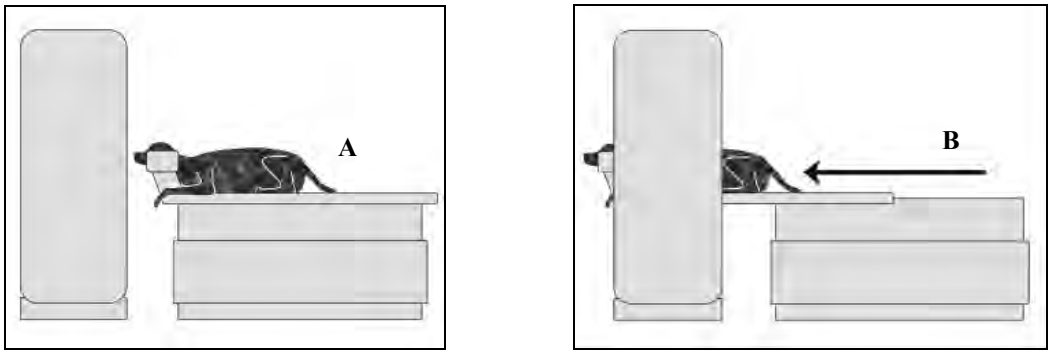

Fig. 6 Illustration of a CT scan in progress. The patient can be moved through the aperture in a series of small increments (i.e. axial scan mode) or continuously (i.e. helical scan mode) (WHATMOUGH, 2006).

2.3.3.2.2 Image Interpretation

A thorough knowledge of normal anatomy is essential, certainly when dealing with cross sectional images. Interpretation is simplified in some areas of the body by comparing to the opposite side. Straight standardized positioning produces symmetric anatomy on transverse images, making interpretation much easier (HATHCOCK and STICKEL, 1993). The identification of structures on one transverse image can usually be accomplished simply by examining multiple adjacent transverse images. The scanned structure can be followed in relation to recognizable surrounding organs as it appears

and disappears. With its image based on the differential absorption of the x-ray beam by different tissues, CT provides a far better soft tissue resolution than conventional x-rays. Lesions are detected by virtue of displacement or deformity of normal landmarks (mass effect) or by changes in tissue density due to pathological processes such as edema, hemorrhage, necrosis, calcification and osteolysis. External landmarks and depth measurements are used to localize lesion for the purpose of biopsy, surgery or radiotherapy. Appropriate window levels and window widths are crucial for the proper interpretation of CT images and must be adapted to the tissue type and area of interest (DENNIS, 1996). Image manipulation can be done after the exposure as the image is on the display screen. Prior to making a printed copy of the CT scan, the correct density and contrast must be selected. Regions of interest (ROI) can be selected and various data computed and displayed regarding them, including size and CT number average and range. Comparison of CT numbers between different areas on an image is sometimes useful, particularly regarding to relative differences in density (HATHCOCK and STICKEL, 1993).

2.3.3.2.3 Computer Tomography in Canine Elbow Dysplasia

Computed tomography has a high accuracy for diagnosis of a fragmented medial coronoid process (FMCP). The advantages of CT over conventional radiography include the following: depiction of detailed cross-sectional anatomy without distraction from superimposed structures, thereby decreasing the complexity of the image, variation in gray scale formats, and enhanced contrast resolution and computer reconstruction of multiplanar images (BRADEN et al., 1994; REICHLE et al., 2000; RING et al., 2002; ROVESTI et al., 2002).

Besides the clinical signs, the diagnosis is mostly made on the basis of the radiographic examination of the patients. Unfortunately, the radiographic findings may not be conclusive, and in most instances the lesions can only be indirectly diagnosed by the appearance of a new bone proliferation. These osteophytes are the signs of a secondary DJD, and they do not appear until the dog is about 7 to 8 months old. The ideal situation, however, would be that FMCP, OCD, or both within the elbow joint could be directly diagnosed before the radiographic appearance of DJD changes, which are signs of joint damage (REICHLE et al., 2000; KORBEL et al., 2001). The results of the study by DE RYCKE et al. (2002) indicate that by the use of CT, not only can bony structure be evaluated, but that with the correct window settings a detailed observation of muscular, tendons, vascular, and even some nervous tissue structure is possible. By studying the axial computed tomography images, the complexity of the radiographic images can be reduced, although some familiarization with this type of imaging is necessary. Use of CT offers the advantages of evaluating the medial coronoid process and the medial part of the humeral condyle in detail and without superimposition of bony structures (BRADEN et al., 1994; REICHLE et al., 2000; RING et al., 2002; ROVESTI et al., 2002). Fragmentation of the coronoid process is easy to recognize on computed tomographic images (KORBEL et al., 2001). It is unquestionable that CT evaluation of the elbow joint has been shown to have high sensitivity and specificity for diagnosis of FMCP (CARPENTER et al., 1993; GIELEN, 2003).

CT has been published as a diagnostic tool for investigation of elbow incongruence. BOULAY (1998) demonstrated an increase in the humero-ulnar joint space at the center of the trochlear notch in one affected bone. Sagittal and coronal plane images can be constructed from transverse CT scans. These images provide good visualization of

elbow joint surface (REICHLE et al., 2000; De RYCKE et al., 2002; HOLSWORTH et al., 2005) and useful for measuring radio-ulnar incongruence (HOLSWORTH et al., 2005). The accuracy of reconstructed CT for joint space measurement is studied by GEMMILL et al. (2005). He stated that the measurement of humero-radial and humero-ulnar joint space could be reliable. Furthermore, he compared normal elbow and elbow-affected medial coronoid disease and incongruence. His results showed the diseased elbow had widening of the humero-radial joint space more than the normal elbow joint. The study also stated that although radio-ulnar incongruence existed at the level of coronoid apex no incongruence was apparent at the level of the coronoid base (GEMMILL et al., 2005). In contrast, KRAMER et al. (2006) found that incongruence was identified at the level of the base, more than at the apex. The difference in the level of the incongruence may result from differences in the measurement technique used or a different cohort of dogs (GEMMILL and CLEMENTS, 2007). The major disadvantage of CT is the requirement of general anesthesia, and maintenance costs of the equipment are high. In addition, in the old generation of CT the overall examination time is more than 10 minutes (DE RYCKE et al., 2002).

2.3.3.3 Arthroscopy

2.3.3.3.1 Principles

Prof. Kenji Takagi of Tokyo University was the first one who successfully applied the principles of endoscopy to a knee joint of a human being in 1918. Arthroscopy in the dog was first reported in 1978 (SIEMERING, 1978). Since that time, the use of arthroscopy in small animal surgery has gained more popularity. Arthroscopic procedures have been employed for diagnostics and therapeutics for the shoulder (PERSON, 1989; VAN RYSSEN et al., 1993; ROCHAT, 2000; BEALE et al., 2003,

BARDET, 1998, BARDET, 1999), elbow (VAN RYSSEN and VAN BREE, 1993; BARDET, 1997; SAM, 2000), stifle (KIVUMBI and BENNETT, 1981; BERTRAND et al., 1997;), and hock (VAN RYSSEN and VAN BREE, 1993; ROCHAT, 2001, BEALE et al., 2003,). There are a variety of sizes and angles of arthroscopes. The diameter of the arthroscope is important in providing the rigidity needed to prevent bending. If the arthroscope is bent, it alters the path of the light beams, which can affect the resolution of the image (DUKES, 1997). Arthroscopes are available in various external diameter sizes, including 1.7 mm, 2.2 mm, 2.7 mm, 3.5 mm, with a wide variety of scope canular size as well. The 2.7 mm arthroscope is commonly employed in small animal veterinary surgery due to the small size of canine joints. Larger arthroscopes are used in larger joints that require manipulation within the joint and that provide more space (DUKES, 1997). However, the effective field of vision of smaller arthroscopes can be increased by having the end optic of scope offset at an angle and by rotation of the scope within the joint about its longitudinal axis. The angle scope offset is called the foreoblique angle and can be defined as the angle between the long axis of the arthroscope and the center of the field of projection (BEALE et al., 2003). An advantage of the angle arthroscope is that the field of projection can effectively be increased by rotating the arthroscope (DUKES, 1997). Although larger angles could potentially increase the field of vision, the greater the angle, the more difficult the image becomes to orient. A 25 to 30 degree foreoblique angle is most often used in veterinary surgery and provides an adequate intra-articular view. Arthroscope attached to an eyepiece (direct-viewing scope) is available, but scopes with camera attachments and viewing monitors are more commonly employed since they are easier to use. Unlike endoscopy, in which resolution is limited by the human eye, video imaging is limited by the video chip or pixel or by the monitor resolution (DUKES, 1997). Additionally, arthroscope can operate with a

variety of light sources. Light sources provide illumination within the joint for visualization. The light source box contains the lamp and intensity regulators. Lamps may be tungsten, metal halide, and xenon listed in order of increasing intensity and usefulness. Tungsten bulbs are the least expensive, but are also the least powerful. The color range for this light source is in the yellow-orange and it operates at 150 watts. Metal halide bulbs run at 300 watts with a much whiter light. However, they are more expensive than the tungsten light sources. Xenon light sources are the most powerful sources. They provide the most accurate color definition and run at 30 watts, but it is the most expensive sources (GURVIS, 1987; BEALE et al., 2003).

Fluids or gas (CO_2 or N_2O) may be applied for joint distension (ERIKSSON and SEBIK, 1982). Fluid pumps permit precise control over flow rate, inflow pressure, and, in some cases, outflow rate (BEALE et al., 2003). Disadvantages of fluid pumps include their initial cost and the cost of the administration sets, the moderate complexity of tube setup, and the space requirements (BEALE et al., 2003). Fluid joint distension systems are most commonly employed in human orthopedics, and besides experimentally always employed in veterinary surgery (VAN BREE and VAN RYSSEN, 1998). Gas distension has the advantage of a larger field of projection and sharp delineation of details. However, gas distension requires special equipment. The disadvantages of gas distension are: hemorrhage can obscure the field of projection, and post-operative periarticular emphysema can develop (PERSON, 1986).

In veterinary surgery, an arthroscopic procedure begins with sterile preparation of the affected limb. The joint is generally distended with a balanced electrolyte solution prior to scope insertion. Some surgeons prefer to place bupivacaine and/or epinephrine within

the solution to aid in pain control and hemorrhage, respectively. After joint distension, the arthroscope and arthroscopic instruments are placed within the joint through portals created with blunt or sharp trocars. Arthroscopic surgery is generally performed using a triangulation technique. This technique requires the arthroscope be placed in one area of the joint, the cannular system and other instruments are in another area like a triangle. This triangle should be formed between the field of projection and the instrument portals. This technique increases maneuverability and optimizes the projection (VAN BREE and VAN RYSSEN, 1998; BUBENIK, 2002; BEALE et al., 2003,).

2.3.3.3.2 Complications

The most common complications associated with arthroscopy surgery are extravasations of fluid into the tissues surrounding the joint, fluid accumulation outside the joint are a minor complication. It is completely absorbed within 24 hours. Fluid extravasations cause collapse of joint capsule into the joint (BEALE et al., 2003). The other disadvantages are obstruction of the visual field by intra-articular elements and hemorrhage, infection, pain, seroma, cartilage scarification, trauma to periarticular soft tissues resulted from difficult arthroscope insertion, inability to correct the patient's problem without additional arthrotomy, and iatrogenic instrument damage (KIVUMBI et al., 1981; PERSON, 1989; VAN RYSSEN and VAN BREE, 1993; SCHWARZ et al., 1997). In human medicine, iatrogenic nerve damage is also a concern, but that has not been reported in veterinary medicine (BUBENIK, 2001).

The other serious complication during arthroscopic procedures is iatrogenic cartilage damage from arthroscope insertion. Most procedures cause minor abrasion of the surface. These abrasions do not lead to degenerative arthritis (BEALE et al., 2003). The

healing of articular cartilage following arthroscope scarification has been evaluated. This study evaluated the healing of articular cartilage over a four week time period. Superficial lesions smoothed, but did not completely heal during this time. Deeper lesions also showed superficial smoothing, but they typically filled in with fibrocartilage. With insertion of the scope into canine stifle joints, the tip of the arthroscope created only superficial lesions, and these lesions showed little, if any, inflammatory reaction (KLEIN, 1986). The risk of severe iatrogenic damage is often caused by forcing a large arthroscope into a small joint, or by excessive movement of the arthroscope tip within the joint, or by inappropriate movement within intra-articular instruments (BEALE et al., 2003).

2.3.3.3.3 Advantages and Disadvantages

Enhanced visualization, lower patient morbidity rates, and increased precision are offered by arthroscopy. Although arthroscopy is a minimally invasive technique it allows an extended and a detailed inspection of the joint. The intra-articular structures and their pathologic changes can be inspected very accurately because of the close inspection, the enlargement by arthroscope and camera, and the suspension of the structures in the irrigation fluid. Fibrillation and superficial erosions of cartilage, fibers of (partially) ruptured ligaments, and the capillary vascularisation of synovial villi are details that cannot be appreciated during an arthrotomy. These possibilities allow a better understanding of the intra-articular anatomy and pathology. Arthroscopy can be used to demonstrate very discrete or early lesions without radiographic evidence. It allows a minimal invasive exploration of joints with severe arthrosis and of joints that have been treated unsuccessfully via arthrotomy or arthroscopy. Decreasing post-operative pain with arthroscopically assisted joint surgery is well documented in human

medicine. Because of the minimal surgical trauma, there is little post-operative care and minimal risk of complications. In case of osteochondritis dissecans, bilateral treatment can be performed during one anesthesia (ABERCROMBY, 1997; McCARTHY, 1999; KAPATKIN, 2003; JANTHUR, 2002, BEALE, 2003). Although the advantages of arthroscopically assisted surgery are superior to the disadvantages, some important disadvantages should be warranted. Skilled and trained veterinarians are required to manipulate the arthroscope and instrumentation within the joint without causing iatrogenic injury to cartilage surface. A second disadvantage is the expensive cost associated with obtaining and maintaining the necessary equipment and instrumentation. The equipment is fragile and easy to damage, therefore, proper training of the technical staff in the handling, sterilization, and storage of equipments are essential (BEALE et al., 2003; CAPALDO et al., 2005).

2.3.3.3.4 Elbow Joint Arthroscopy

Arthroscopy of the cubital joint in small animal surgery is rapidly growing in popularity. In 1993, VAN RYSSEN and VAN BREE evaluated a medial approach to the cubital joint in dogs. The arthroscope was inserted caudo-distal to the medial epicondyle of the humerus. Cadaver studies found that the trocar for arthroscope placement passed through or between the muscles of the deep digital flexor and superficial digital flexor and that minimal cartilage damage occurred with arthroscope insertion at that site. Neurovascular injury was not noted. Additionally, animals were minimally affected, minimally lame, and there were minimal problems with the surgical site by the procedure, and visualization was adequate for evaluation of the medial aspect of the cubital joint.

BARDET (1997) also reported on a craniolateral approach to the cubital joint. In this approach, the arthroscope was placed craniolateral to the lateral humeral epicondyle. All the medial structures of the joint could be visualized; however, the lateral component of the cubital joint could be visualized more readily than with the medial approach. With this approach, the trocar passed cranial to the pronator teres muscle or through the insertion of the teres muscle. Again, no neurovascular damage was noted and minimal cartilage damage was visualized. Both the medial and craniolateral approach provide adequate exposure of the cubital joint for arthroscopic procedures. The medial approach is most commonly employed in veterinary surgery due to superior exposure of the medial aspect of the joint, where clinical problems occur commonly in small animals.

Cartilage lesion can be easily graded arthroscopically (NESS,1998) and an arthroscopic technique allows good inspection of canine elbow joint, with minimal tissue damage and rapid recovery (VAN RYSSEN et al., 1993). The coronoid process and medial humeral condyle can be evaluated in detail (VAN BREE and VAN RYSSEN, 1995). In comparison with the non-specificity of the radiographic findings, arthroscopy allows a specific evaluation of joint lesions. Different types of lesions in the area of the coronoid process can be differentiated arthroscopically, such as chondromalacia-like lesions, fissures of the articular cartilage and displaced-, non-displaced fragments containing subchondral bone (BARDET, 1997, VAN BREE and VAN RYSSEN, 1995). Moreover, ‘kissing lesion’ and OCD lesion on the medial humeral condyle, arthrotic changes and inflammation of the synovial membrane can also be evaluated (VAN BREE and VAN RYSSEN, 1995). Arthroscopy can allow identification of incongruence (BEALE et al., 2003; FITZPATRICK, 2004), although the reliability of the technique has been

questioned, as the introduction of the arthroscope into the elbow may induce or disguise the presence of incongruence (GEMMILL and CLEMENT, 2007).

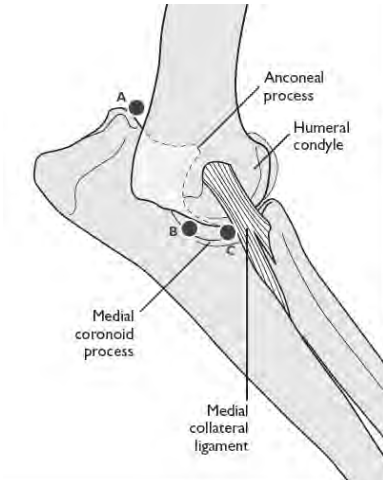

A

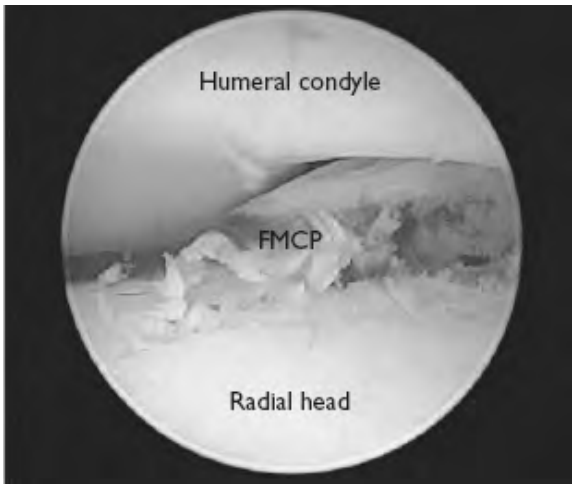

B

Fig. 7 (A) Medial projection of portal locations and pertinent anatomy for canine elbow arthroscopy: A—Infusion and egress portal, B—Arthroscope portal, C—Instrument portal (B) Arthroscopic projection of a fragmented medial coronoid process. (CAPALDO, 2006)

2.3.4 Treatment of Canine Elbow Dysplasia

Treatment for FMCP includes non-surgical management and surgery (LEWIS et al, 1992; HUIBREGSTE et al., 1994; TOBIAS et al., 1994; BOUCK et al., 1995; MEIJ et al., 1996; BRUNNBERG, 1996; COOK, 1997; BOULAY, 1998; NESS, 1998; THEYSE, 2000;). Non surgical management includes weight control (KEALY, 2000), activity restriction (READ, 1987) and medication for pain and osteoarthritis (READ, 1987), physical therapy (CONZEMIUS, 2004) and the use of slow acting agents such as glucosamine, chondrotin, polysulphated glycosaminoglycans and pentosan polysulphate (BOUCK, 1995). The goal of surgery includes removal of loose or free floating cartilage or bone fragments and correction of articular incongruence (LEWIS et al., 1989; BOULAY, 1998). Typical surgical procedures are medial arthrotomy and arthroscopy (DENNY, 1980; READ, 1990; PIERMATTI, 1997; VAN RYSSEN and VAN BREE, 1997; BARDET, 1997; MEYER-LINDENBERG, 2003).

The results of surgical management are unsatisfied. Many researchers indicated that most dogs develop osteoarthritis after surgery (BENNETT, 1981; HUIBREGSTE et al., 1994; THEYSE et al., 2000). Generally, surgery is not only recommended for dogs younger than 12 months of age that have clinical or radiographic signs of FMCP but also for dogs up to 24 months with large lesions evident radiographically and significant clinical signs (LEWIS, 1992). Dogs with severe osteoarthritis are better with conservative therapy. The prognosis for dogs with FMCP varies and depends on the severity of clinical signs, progression of osteoarthritis, and treatment used (TROSTEL et al., 2003). Treatments of elbow incongruity are problematic and depend on the cause and severity of the incongruity. A variety of osteotomy has been described, proximal ulnar osteotomy (THOMPSON and ROBBINS, 1995; BARDET and BUREAU, 1996; NESS, 1998; PRESTON et al., 2001), radial osteotomy (SLOCUM and PFEIL, 2004). However, GEMMILL et al. (2005) stated that the correction of incongruence by osteotomy at one level may induce a subsequent incongruence at another level, thus it could lead to further problems. Later in the disease, after bony formation surgical treatment may be ineffective. The good treatment option may include long-term medical treatment, arthrodesis, total elbow arthroplasty, and amputation (CONZEMIUS et al., 2003, TROSTEL et al., 2003).